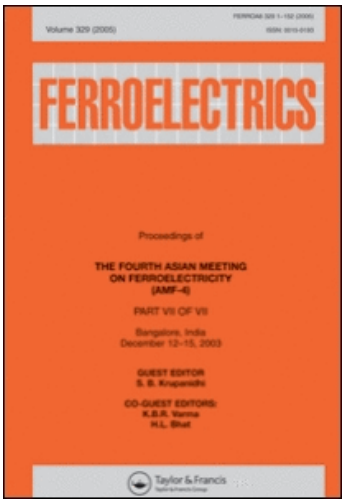

Ferroelectrics
Publication details, including instructions for authors and subscription information:
http://www.informaworld.com/smpp/title~content=t713617887

Ferroelectric/Antiferroelectric $Pb(Zr_{0.8}Ti_{0.2})O_3/PbZrO_3$ Epitaxial Multilayers: Growth and Thickness-Dependent Properties

Ksenia Boldyreva [a]; Lucian Pintilie [ab]; Andriy Lotnyk [a]; I. B. Misirlioglu [a]; Marin Alexe [a]; Dietrich Hesse [a]
[a] Max Planck Institute of Microstructure Physics, Halle, Saale, Germany [b] NIMP, Bucharest-Magurele, Romania

Online Publication Date: 01 January 2008

To cite this Article Boldyreva, Ksenia, Pintilie, Lucian, Lotnyk, Andriy, Misirlioglu, I. B., Alexe, Marin and Hesse, Dietrich(2008)'Ferroelectric/Antiferroelectric $Pb(Zr_{0.8}Ti_{0.2})O_3/PbZrO_3$ Epitaxial Multilayers: Growth and Thickness-Dependent Properties',Ferroelectrics,370:1,140 — 146

To link to this Article: DOI: 10.1080/00150190802384492

URL: http://dx.doi.org/10.1080/00150190802384492

Ferroelectrics, 370:140–146, 2008

ISSN: 0015-0193 print / 1563-5112 online
DOI: 10.1080/00150190802384492

Taylor & Francis
Taylor & Francis Group

Ferroelectric/Antiferroelectric $Pb(Zr_{0.8}Ti_{0.2})O_3/PbZrO_3$ Epitaxial Multilayers: Growth and Thickness-Dependent Properties

KSENIA BOLDYREVA,[1,*] LUCIAN PINTILIE,[1,2]
ANDRIY LOTNYK,[1] I. B. MISIRLIOGLU,[1]
MARIN ALEXE,[1] AND DIETRICH HESSE[1]

[1]Max Planck Institute of Microstructure Physics, Weinberg 2, D-06120 Halle (Saale), Germany
[2]NIMP, P.O. Box MG-7, 077125 Bucharest-Magurele, Romania

Epitaxial ferroelectric/antiferroelectric $PbZr_{0.8}Ti_{0.2}O_3/PbZrO_3$ multilayers were grown on $SrTiO_3(100)$ substrates, covered with a $SrRuO_3$ (100) bottom electrode and a thin tetragonal $PbZr_{0.2}Ti_{0.8}O_3$ buffer layer, using pulsed laser deposition. Polarization-field, switching current-voltage and capacitance-voltage curves show a mixed antiferroelectric-ferroelectric behavior of the multilayers with an individual layer thickness above 10 nm, but below 10 nm the multilayers show only ferroelectric behavior. Obviously the $PbZrO_3$ layers thinner than 10 nm underwent a transition into the ferroelectric state. An X-ray diffraction θ-2θ scan showed a corresponding orthorhombic-to-rhombohedral transition of the $PbZrO_3$ layers. The observations are discussed in terms of a strain effect.

Keywords Lead zirconate; lead zirconate titanate; epitaxial multilayers; ferroelectric-antiferroelectric

1. Introduction

Epitaxial perovskite-type multilayers such as $SrTiO_3/BaTiO_3$ represent a class of interesting systems with enhanced ferroelectric or dielectric properties. Lead-based perovskite oxide multilayers are expected to have properties different from those of the individual materials they consist of. Coupling phenomena and strain effects between individual layers can result in qualitatively new properties, particularly within multilayers (artificial superlattices) consisting of ultrathin layers. For example, Kanno *et al.* [1] reported on an increase of the dielectric constant of $PbZrO_3/PbTiO_3$ epitaxial multilayers with decreasing thickness of the component layers for the same total thickness of the structure. This behavior was explained in terms of the interlayer strain and electrical interaction of the dipoles at the interfaces. However, the hysteresis loop showed a ferroelectric behavior independent on the thickness of the component layers (2 nm or 40 nm). Only some qualitative observations have been

Received September 19, 2007; in final form March 20, 2008.
*Corresponding author. E-mail: ksenia@mpi-halle.de

made on sol-gel grown, polycrystalline $Pb(Zr_xTi_{1-x})O_3/PbZrO_3$ multilayers in dependence on the annealing conditions [2]. Epitaxial $Pb(Zr_{0.4}Ti_{0.6})O_3/PbZrO_3$ multilayers fabricated by pulsed laser deposition of about 10 nm thickness were recently studied by Bao *et al*. [3].

Here we report on growth, structure and layer thickness-dependent properties of epitaxial $Pb(Zr_{0.8}Ti_{0.2})O_3/PbZrO_3$ (PZT/PZO) multilayers with a PZT/PZO-ratio of 1:1. Ferroelectric/antiferroelectric (FE/AFE) multilayers of type $Pb(Zr_{0.8}Ti_{0.2})O_3/PbZrO_3$ are particularly interesting in view of the small energy difference between the AFE-phase and the FE-phase in PZO [4] and due to the close crystallographic relation between ferroelectric rhombohedral PZT (lattice parameters a = 4.118 Å, $\alpha = 89.73^\circ$) and antiferroelectric orthorhombic PZO (lattice parameters a = 5.88 Å, b = 11.787 Å, c = 8.231 Å). In a first approximation, both materials are pseudocubic with lattice parameters $a_{pc} = 4.12$ Å for PZT and $a_{pc} = 4.14$ Å for PZO (pc-pseudocubic, for PZO see Ref. 5). Thus the misfit between PZT and PZO is about 0.5%.

2. Experiment and Discussions

The multilayers were prepared by pulsed laser deposition (PLD) on (100)-oriented vicinal $SrTiO_3$ (STO) substrates. A KrF excimer laser with a wavelength of 248 nm was used. The STO substrates were chemically etched and thermally annealed in order to obtain step-terrace structures with only one unit-cell height [6]. As bottom electrode a conducting $SrRuO_3$(SRO) epitaxial layer was deposited. A thin tetragonal $Pb(Zr_{0.2}Ti_{0.8})O_3$ buffer layer (5 nm) was deposited on top of the SRO electrode to reduce the misfit between the rhombohedral PZT(80/20) and the bottom electrode. The deposition conditions were optimized separately for all materials. All layers were deposited at 575°C, with an oxygen pressure of 0.1 mbar for PZO and rhombohedral PZT, 0.14 mbar for SRO, and 0.2 mbar for the tetragonal PZT buffer layer. The laser fluence was set to 1.5, 0.9, 1.0 and 1.0 J/cm^2 for depositing PZO, SRO, PZT and the tetragonal buffer layer, respectively. Pt top electrodes were deposited through a stainless steel shadow mask by rf sputtering. Samples for transmission electron microscopy (TEM) were prepared using mechanical and ion-beam based standard thinning methods. TEM investigations were performed in a Philips CM20T at 200 kV. X-ray diffraction (XRD) θ–2θ scans and reciprocal space mappings (not shown) were performed on a Philips X'Pert MRD diffractometer with CuK_α radiation. Polarization-voltage (P-V) hysteresis loops and switching current-voltage (I-V) characteristics of the multilayers were recorded by an AixAcct Thin Film Analyzer 2000. The surface morphology of the substrates (Fig. 1(a)) and the multilayers was studied by atomic force microscopy (AFM), revealing layer-by-layer growth resulting in stepped terraces (Fig. 1(b)).

Single-phase ferroelectric rhombohedral PZT and antiferroelectric orthorhombic PZO single crystals and thin films are well investigated [7–13]. Ferroelectric PZT films show the well-known ferroelectric hysteresis loop. Figure 2(a) shows such a loop for a PZT film of 105 nm thickness [14]. A characteristic double loop is recorded from antiferroelectric PZO films due to a field-induced antiferroelectric-to-ferroelectric transition. Figure 2(b) shows a double loop for a PZO film of 385 nm thickness [8]. During this transition the crystallography of PZO changes from orthorhombic to rhombohedral [15]. Thus the FE-axis of PZO lies along the $[111]_{pc}$ direction, as in rhombohedral PZT.

Three sets of samples $[PZO_t/PZT_t]_m$ with different overall thicknesses $T = 2{\cdot}m \cdot t$ of 50 nm, 100 nm and 150 nm, respectively, were investigated. t is the thickness (in nanometers) of the individual PZT or PZO layers, and m is the number of PZT/PZO bilayers. The results were similar for the three sets of samples. The structure of a multilayer with $T = 150$ nm,

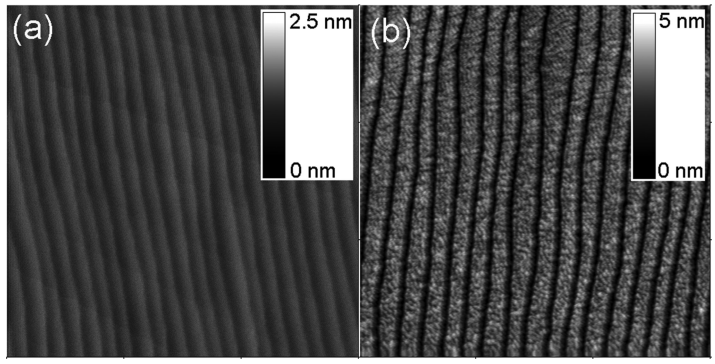

Figure 1. AFM images (3×3 μm) (a) of a STO(100) substrate after chemical and thermal treatment, (b) of a multilayer with overall thickness $T = 100$ nm, consisting of 4 bilayers with $t = 12.5$ nm.

$t = 9$ nm and $m = 8$ is shown in Fig. 3. All the layers grow epitaxially in the pseudocubic (001) orientation, as revealed by selected area electron diffraction (Fig. 4).

The P-V characteristics of $[PZO_t/PZT_t]_m$ multilayers with $T = 100$ nm, but different number of bilayers ($m = 1$, 2, 4, 6 and 8), corresponding to $t = 50$, 25, 12.5, 9 and 6 nm, respectively, were measured. The samples with $t = 50$, 25 and 12.5 nm show a mixed FE-AFE behavior, but the samples with $t = 9$ and 6 nm show only FE behavior. Figure 5a shows the hysteresis loops for the t values of 25 nm and 6 nm ($m = 2$ and $m = 8$), respectively. The mixed FE-AFE behavior in the case of $t = 25$ nm is clearly visible in the switching I-V curve shown in Fig. 5(b). Two additional switching peaks (encircled) are present near zero bias, in addition to the four antiferroelectric major switching peaks (marked with arrows). The sample with $t = 6$ nm, however, shows only two peaks, indicating the purely FE behavior. Thus the PZO layers undergo a thickness-driven transition from an AFE behavior to a FE behavior at a certain critical thickness t_c between 9 and 12.5 nm.

The effect of a thickness-driven phase transition also showed up in C-V curves. The multilayer with $t > t_c$ showed a mixed AFE-FE behavior, whereas at $t < t_c$ only a FE behavior was observed (Fig. 6). Calculating the dielectric constant from capacitance and representing it as a function of thickness t, a maximum in the curve was observed at $t = 9$–10 nm [16]. Similar to the maximum of the dielectric constant at a phase transition temperature, this maximum at t_c supports the conclusion on a thickness-driven phase transition.

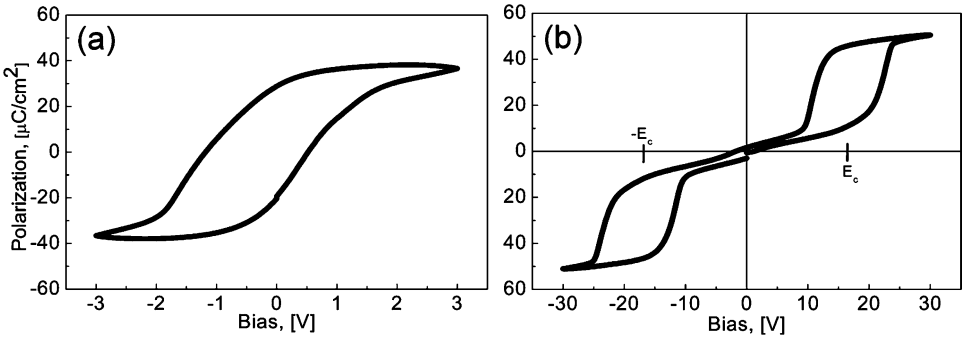

Figure 2. P-V hysteresis for (a) a 105 nm thick ferroelectric PZT film and (b) a 385 nm thick antiferroelectric PZO film.

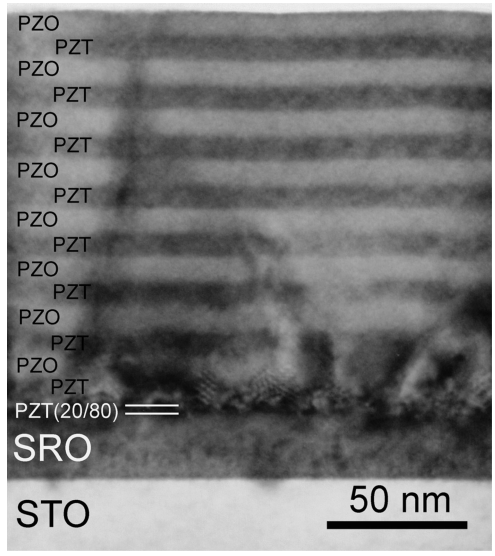

Figure 3. TEM cross-section image of a multilayer with an overall thickness of 150 nm, a number of bilayers $m = 8$ and an individual layer thickness of $t = 9$ nm. (PZT – $Pb(Zr_{0.8}Ti_{0.2})O_3$).

Figure 7 shows part of a XRD θ–2θ scan near the peaks of fourth order ($\psi = 0^\circ$) for two multilayers with $t = 25$ nm and $t = 6$ nm. The sample with $t = 25$ nm shows two peaks at $2\theta = 95.35^\circ$ (d-value 1.0419 Å) and 96.42° (d-value 1.0331 Å) corresponding to the PZO $(480)_o$ and PZT $(004)_{rh}$ reflections (o-orthorhombic and rh-rhombohedral), respectively. The latter sample, however, shows only one peak at $2\theta = 96.11^\circ$ (d-value 1.0356 Å), which indicates

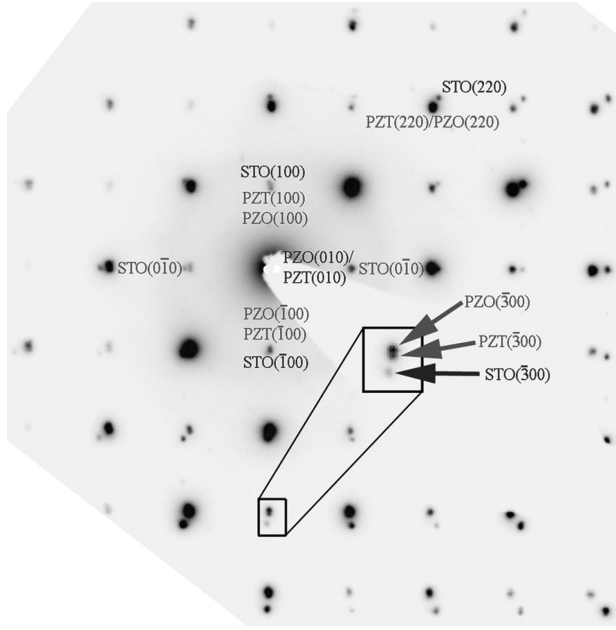

Figure 4. Selected area electron diffraction of a multilayer with $t = 25$ nm and $m = 2$ [14].

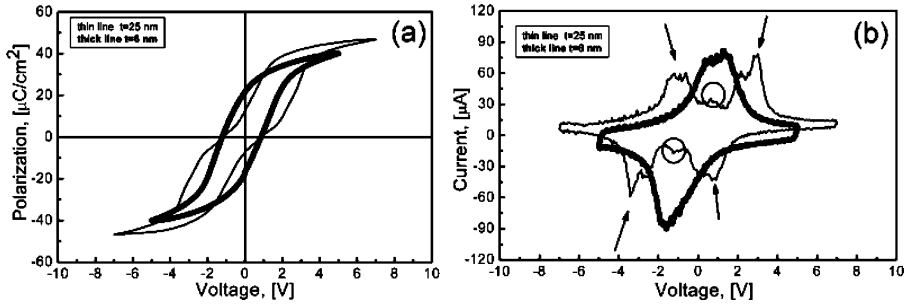

Figure 5. (a) P-V hysteresis loops and (b) switching current-voltage curves for two multilayers with $t = 25$ nm and $t = 6$ nm ($m = 2$ and $m = 8$), respectively.

a somewhat strained, uniformly *rhombohedral* phase. In other words, PZO has undergone a structural phase transition from orthorhombic to rhombohedral at $t_c = 10$ nm, which is equivalent to the observed AFE-to-FE transition in the P-V and I-V curves. The structural transition has been even more clearly illustrated by XRD reciprocal space maps [16]. In result, in a pseudocubic approximation the sample with $t = 25$ nm consists of PZO layers with $a_{pc} = 4.17$ Å and PZT layers with $a_{pc} = 4.13$ Å, so that the PZO is under compressive, the PZT under tensile strain. After the structural phase transition both PZO and PZT have a pseudocubic lattice parameter $a_{pc} = 4.14$ Å, indicating that strain plays a significant role as an origin of the thickness-driven antiferroelectric-to-ferroelectric transition of the very thin PZO layers.

Regarding the origin of the structural phase transition in the thin PZO layers, one should remember that the component materials of the multilayers have different paraelectric-to-(anti)ferroelectric transition temperatures. During growth at 575°C, all the layers have a cubic structure and grow cube-on-cube. Taking for simplicity the transition temperatures of the bulk, the paraelectric-to-ferroelectric (cubic-to-rhombohedral) transition of the $PbZr_{0.8}Ti_{0.2}O_3$ layers occurs at $T_c = 317$°C, and the paraelectric-to-antiferroelectric (cubic-to-orthorhombic) transition of the PZO layers at $T_c = 230$°C. In the temperature range between 317°C and 230°C, the PZO layers are expected to be still cubic and paraelectric, whereas the PZT layers are rhombohedral and ferroelectric. The correspondingly occuring

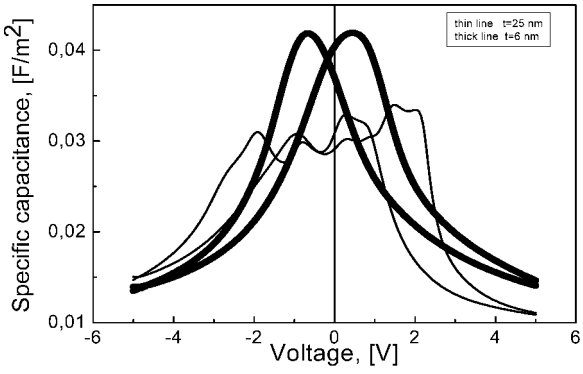

Figure 6. C-V characteristic of the two multilayers with $t = 25$ nm (thin line) and $t = 6$ nm (thick line).

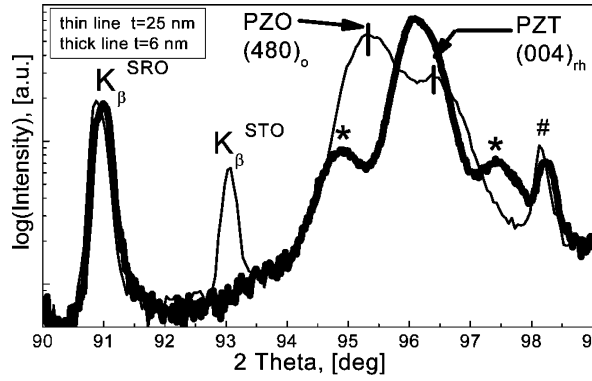

Figure 7. Part of a XRD θ-2θ scan of two multilayers with $t = 25$ nm and $t = 6$ nm. The two reflections marked with an asterisk are second-order superlattice reflections corresponding to a PZT/PZO layer period of 13.4 nm. Diffraction from the tetragonal $PbZr_{0.2}Ti_{0.8}O_3$ buffer layer is not seen due to the low thickness of this layer (5 nm). The symbols "K_β^{STO}" and "K_β^{SRO}" mark the (004) peaks coming from the K_β radiation, and "#" a peak coming from the W_L radiation due to the contamination of the anode by tungsten from the cathode.

polarization charges at the interfaces may in principle induce an electric field in the PZO layers in addition to the strain. Perhaps this field assists to drive the PZO layers towards the rhombohedral, ferroelectric, phase, if the individual layer thickness is thin enough (less than 10 nm). However, due to the very small free energy difference between the AFE and FE phases in PZO [16] (as it was already shown for bulk and thin films [7, 18]), stress alone may be sufficient to drive the transition. More investigations, including also Monte-Carlo simulations, are being performed to better understand the details of the mechanism of the thickness-driven phase transition.

3. Conclusion

In conclusion, a thickness-driven antiferroelectric-to-ferroelectric, orthorhombic-to-rhombohedral phase transition of very thin $PbZrO_3$ layers in epitaxial ferroelectric/antiferroelectric $PbZr_{0.8}Ti_{0.2}O_3/PbZrO_3$ multilayers has been observed at a $PbZrO_3$ thickness below 10 nm. The transition is most probably a result of interfacial strain occurring during cooling down the samples after the growth at high temperature.

Acknowledgments

Thanks are due to M. A. Schubert for help with some XRD measurements. One of the authors (I. B. M.) thanks the Alexander von Humboldt Foundation for funding.

References

1. I. Kanno, S. Hayashi, R. Takama, and T. Hirao, *Appl. Phys. Lett.* **68**, 328 (1996).
2. S. H. Bae, K. B. Jeon, and B. M. Jin, *Mat. Res. Bull.* **36**, 1931 (2001); S. H. Bae, K. B. Jeon, B. M. Jin, and I. W. Kim, *Ferroelectrics* **260**, 113 (2001); S. H. Bae, K. B. Jeon, S. C. Kim, and B. M. Jin, *Ferroelectrics* **260**, 131 (2001); S. H. Bae, K. B. Jeon, and B. M. Jin, *Ferroelectrics* **328**, 9 (2005).

3. D. H. Bao, R. Scholz, M. Alexe, and D. Hesse, *J. Appl. Phys.* **101**, 054118 (2007).
4. E. Sawaguchi, *J. Phys. Soc. Jpn.* **8**, 615 (2007).
5. F. Jona, G. Shirane, F. Mazzi, and R. Pepinsky, *Phys. Rev.* **105**, 849 (1957).
6. G. Koster, B. Kropman, G. Rijnders, D. Blank, and H. Rogalla, *Appl. Phys. Lett.* **73**, 2920 (1998).
7. M. P. Moret, J. J. Schremer, F. D. Tichelaar, E. Aret, and P. R. Hageman, *J. Appl. Phys.* **92**, 3947 (2002).
8. K. Boldyreva, D. Bao, G. Le Rhun, L. Pintilie, M. Alexe, and D. Hesse, *J. Appl. Phys.* **102**, 044111 (2007).
9. D. Viehland, *Phys. Rev. B* **52**, 778 (1995).
10. D. L. Corker, A. M. Glazer, R. W. Whatmore, A. Stallard, and F. Fauth, *J. Phys.: Condens. Matter* **10**, 6251 (1998).
11. S. K. Streiffer, C. B. Parker, A. E. Romanov, M. J. Lefevre, L. Zhao, J. S. Speck, W. Pompe, C. M. Foster, and G. R. Bai, *J. Appl. Phys.* **83**, 2742 (1998).
12. K. Tokita, M. Aratani, and H. Funakubo, *Ferroelectrics* **260**, 45 (2001).
13. D. I. Woodward, J. Knudsen, and I. M. Reaney, *Phys. Rev. B* **72**, 104110 (2005).
14. K. Boldyreva, *PhD Thesis*, Martin Luther University Halle-Wittenberg (2007).
15. O. E. Fesenko, R. V. Kolesova, and Yu. G. Sindeyev, *Ferroelectrics* **20**, 177 (1978).
16. K. Boldyreva, L. Pintilie, A. Lotnyk, I. B. Misirlioglu, M. Alexe, and D. Hesse, *Appl. Phys. Lett.*, **91**, 122915 (2007).
17. E. Sawaguchi, *J. Phys. Soc. Jpn.* **8**, 615 (1953).
18. V. Yu. Topolov, A. V. Turik, O. E. Fesenko, and V. V. Eremkin, *Ferroelectr. Lett. Sect.* **20**, 19 (1995).